Bulletin of Electrochemistry 12 (3-4) Mar-Apr 1996, pp 213-217

0256-1654/96/$ 3-50

IRON-COPPER ELECTRODES FOR ALKALINE BATTERIES

G PARUTHIMAL KALAIGNAN AND V S MURALIDHARAN*

Department of Industrial Chemistry, Alagappa University, Karaikudi 630 003. INDIA

* Central Electrochemical Research Institute, Karaikudi 630 006. INDIA

Alkaline Ni-Fe batteries employ sintered iron electrodes as anodes. Iron oxide and copper powders are added to iron powder during sintering to improve charge retention and cycle life. Electrochemical studies on the iron-copper electrodes revealed that iron oxide addition hindered the formation of higher valent oxides of iron and reduced the self discharge. An optimum composition of iron oxide and copper for iron electrodes has been suggested.

Keywords: Nickel-iron battery, sintered iron electrode, alkaline iron electrode and iron-copper electrode

INTRODUCTION

Sintered porous iron electrodes are used in the Ni-Fe cell to have long cycle life. To increase the hardness strength and conductivity, copper powder is incorporated in the sintered iron electrode [1]. Inclusion of copper powder favours uniform pore size distribution and lowers the sintereing temperature of the electrode [2,3]. When copper is added upto 20%, pressed Fe(III) oxides exhibited better utilisation. The present work is aimed to understand the electrochemical bahaviour of sintered Fe-Cu electrodes in 6.0 *M* KOH + 0.63 *M* LiOH with a view to develop a battery electrode with high charge retention.

EXPERIMENTAL DETAILS

Preparation of porous iron electrode

Iron powders of different origins with different properties were used for the electrode preparation (Table I). Iron powder was reduced at 573 K for two hours in hydrogen atmosphere. Loose sintered electrodes were prepared from iron powder and the mixtures of Fe, Fe_3O_4 and Cu using a number 10 nickel mesh grid of 0.1 mm thick (area 1.67 cm^2, thickness - 2mm) in a graphite die. The electrode was sintered at 1173K for one hour in N_2 atmosphere. The amounts of Fe^{2+} and Fe^{3+} ions in Fe_3O_4 were estimated [4]. Details of the experimental setup for triangular potential sweep voltammetry (TPSV) and gasometric studies have been described eariler [5].

Potential step method and solution analysis

The electrodes were kept at constant potential -0.9, -0.775, -0.525 and -0.29 V for one hour. After the experiments the solutions were analysed using atomic absorption spectrophotometer (Perkin Elmer 380, USA).

Experiments in duplicate were carried out at 303 ± 0.01 K using analar chemicals dissolved in double distilled water. The electrolyte 6 *M* KOH + 0.63 *M* LiOH was deoxygenated by bubbling purified H_2 for one hour. Potentials were measured against Hg/HgO electrode and no corrections were made for liquid junction poentials.

RESULTS

A porous (Fe + 3% Cu) electrode was kept at -1.3 V for 5 min., disconnected, shaken free of attached H_2 bubbles and then polarised from -1.3V to -0.2V (Fig. 1). In the forward scan ZCCP (Zero current crossing potential) occurs at -1.03 V followed by a plateau around -0.9V (I), an anodic peak at -0.825V (II), a shoulder around -0.7V (III), a peak at -0.64V (II) a complete passive region from -0.56V to -0.42V (V) and a sharp peak at 0.325V (VI). The backward scan exhibits a passive region from - 0.2V to -0.55V a sharp peak at -0.94 V (VIII) and peak at-1.1V (IX). Hydrogen evolution was noticed at -1.2V. Increase of scan number reduces the amounts of charge under peaks II, IV and IX increases those for VI, VII and VIII.

This suggests that peaks II and IX belong to a redox couple while the peaks VI, VII and VIII are consecutive.

Introduction of Fe_3O_4 to this electrode slightly modified the spectrum (Fig. 2). During the forward scan ZCCP occurs at -1.035V followed by a plateau around -1.0V (I) and anodic peaks at -0.8V (II), -0.585 V (III) and -0.325 V (IV). During the reverse scan cathodic peaks appear at -0.75V (V), -0.975 V (VI) and -1.140V (VII). Hydrogen evolution takes place at -1.225V. On repeating the polarisation for a few more cycles the reversibility was found to be increased.

Presented in the Fifth International Symposium on Advances in Electrochemical Science and Technology, Madras

TABLE I: Properties of powders used

Powder	Chemical composition	Apparent density g/cc	Tap density g/cc	Particle size	Specific area* m^2/g
Electrolytic iron	99% Fe, 0.001% Pb, 0.008% Zn, 0.001% As, 0.025% Mn, 0.005% Cu	2.84	3.08	≤ 37	11.08
Water atomised iron (ASC 200)	98% Fe, 0.01 % C, 0.007% S, 0.007% P	2.8 to 3.0	—	92% < 60%	18.52
Sponge iron (MH 300.25)	98% Fe, 0.01% C, 0.007% S, 0.007% P	2.75 to 2.95	—	80% < 44% and 20% between 75 and 44	14.00
Synthetic black iron oxide Fe_3O_4	96 to 99% Fe_3O_4 Fe^{2+} = 44.55% Fe^{3+} = 25.73%	1.22	1.71	≤ 37	38.72
Electrolytic copper	99.5% Cu	—	—	≤ 37	14.21

* *Quantasorb using liquid* N_2

Gasometric studies

The self discharge of the iron electrode is cuased by local action accompanied by H_2 evolution. The self discharge current was calculated from the rate of H_2 evolution. The electrode was polarised cathodically at five different potentials and the rate of H_2 evolution was monitored. The

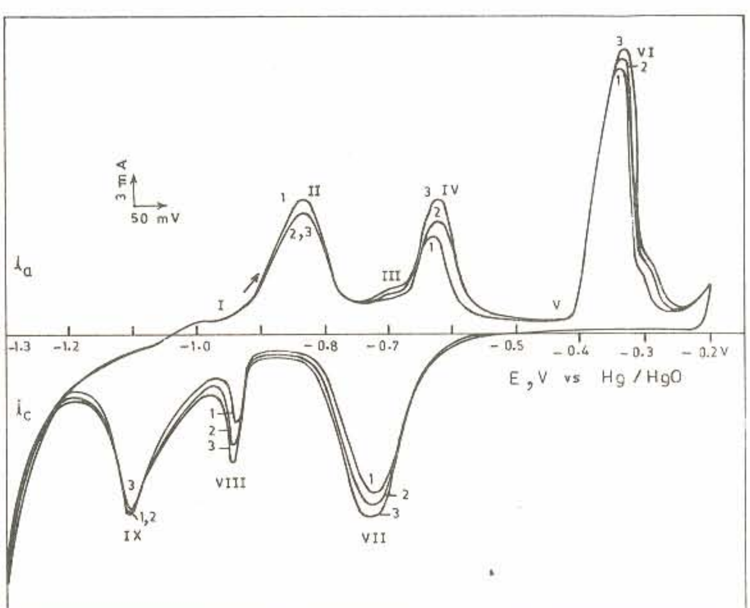

Fig. 1: Typical cyclic voltammogram for porous electrolytic iron powder + 3% Cu electrode in 6 M KOH + 0.63 M LiOH solutions with various scan numbers
$E_{\lambda,c} = -1.3v$; $E_{\lambda,a} = -0.2v$; $v = 1\ mVs^{-1}$

linear segment of the polarisation curve was extrapolated to open circuit potential to obtain self discharge current (Fig. 3).

DISCUSSION

Oxidation - reduction processes occuring at the iron electrode surface was reviewed recently [6]. The formation of $Fe(OH)_2$ takes place Via $FeOH^+_{ads}$ and the further oxidation of $Fe(OH)_2$ to FeOOH can take place as [7,8]. $Fe(OH)_2 + OH^-$ =====> $FeOOH + H_2O + e^-$. In 6 *M* KOH solution, $HFeO_2^-$ formation is also envisaged as $Fe(OH)_2$ may be formed via dissolution - precipitation.

The appearance of a plateau around -1.0V is due to the initial oxidation on the surface. The appearance of peak at -0.825V (II) is due to the formation of $Fe(OH)_2$ or $HFeO_2^-$ ion.

The shoulder around -0.7V (III) appears anodic to the E_e of Cu/Cu_2o reaction [9].

$$Cu + 2H_2O \rightleftharpoons CuO_2^{2-} + 4H^+ + 2e^-$$

$$E_e = -1.136 \text{ V vs Hg/HgO}$$

$$Cu^+ + 2H_2O \rightleftharpoons HCuO_2^- + 3H^+ + e^-$$

$$E_e = -1.026 \text{ V vs Hg/HgO}$$

Hence it may be due to the dissolution of Cu via monovalent oxide along with $Fe(OH)_2$.

In order to confirm the dissolution of Cu, an analysis of the solution was carried out at different potentials. Anodic potentials increased the copper ion concentration in solution, while iron content decreased (Table II). Dissolved copper ions were observed only at potentials anodic to -0.775V. The appearance of peak (IV) is due to the complete oxidation of $Fe(OH)_2$ to FeOOH.

Oxidation of copper can occur [10] in two stages with two surface films of distinctly different morphologies and growth mechanisms. A compact layer is formed by solid state growth mechanism followed by the nucleation and growth of the upper layer of individual crystals from solutions. Copper can disolve at -0.7V to give $HCuO_2^{2-}$.

The appearance of the pasive region around -0.5V (V) is due to the formation of the base layer of Cu_2O via

$$Cu \rightleftharpoons Cu^+_{ads} + e^-$$

$$2Cu^+_{ads} \longrightarrow 2Cu^+_{oxide}$$

The monovalent Cu^+ may be present on the pores of the oxide and react with OH^- ions to form Cu_2O.

$$OH^-_{solution} \rightleftharpoons OH^-_{ads}$$

$$OH^-_{ads} \longrightarrow O^{2-}_{oxide\ lattice} + H^+_{solution}$$

$$2Cu^+_{oxide\ lattice} + O^{2-}_{oxide\ lattice} + H^+_{solution} \longrightarrow Cu_2O$$

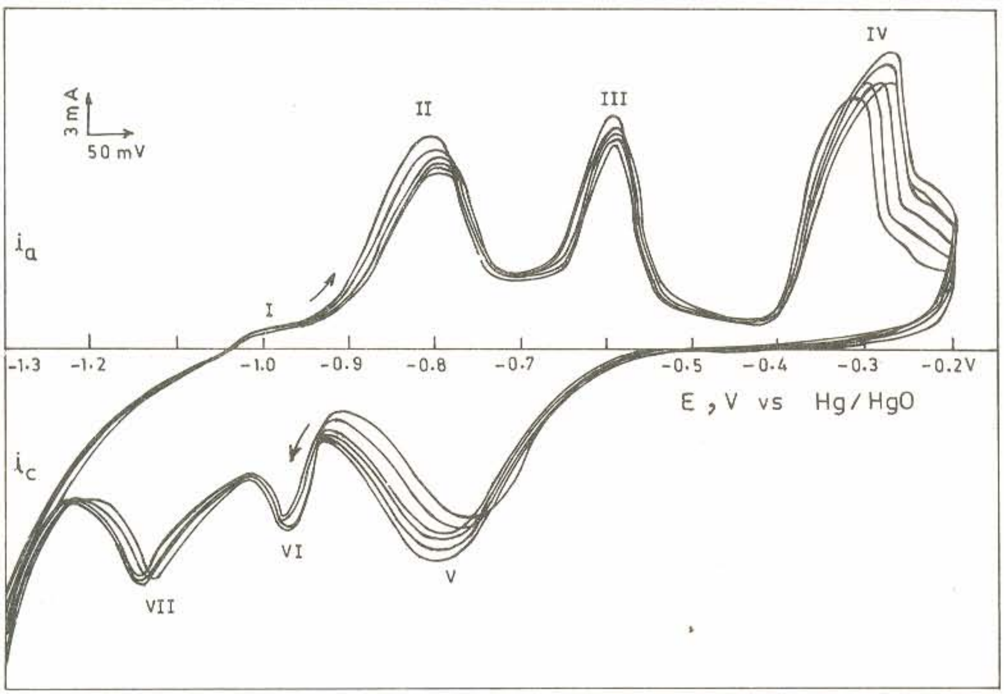

Fig. 2: Typical cyclic voltammogram for porous electrolytic iron + 15% Fe_3O_4 + 3% Cu electrode in 6 M KOH + 0.63 M LiOH solutions with various scan numbers
$E_{\lambda,c} = -1.3v$; $E_{\lambda,a} = -0.2v$; $v = 1\ mVs^{-1}$

This strongly bound layer completely covers the pores of the oxide surface. At potentials -0.4V some part of the Cu_2O may dissolve to yield $[Cu(OH)_n]^{2-n}$ (peak VI).

In the reverse scan the entire surface is covered by Cu_2O while at a potential of -0.6V the appearance of peak VII is due to the irreversible reduction of oxides of copper. The appearance of cathodic peaks at -0.94V (VIII) and peak (IX) at -1.10V is due to the reduction of FeOOH to $Fe(OH)_2$ and then to iron. At high sweep rates, the surface of the electrode participates predominantly in the electrode process. The reduction to copper can also occur from soluble $Cu(OH)_n]^{2-n}$ at higher cathodic potentials.

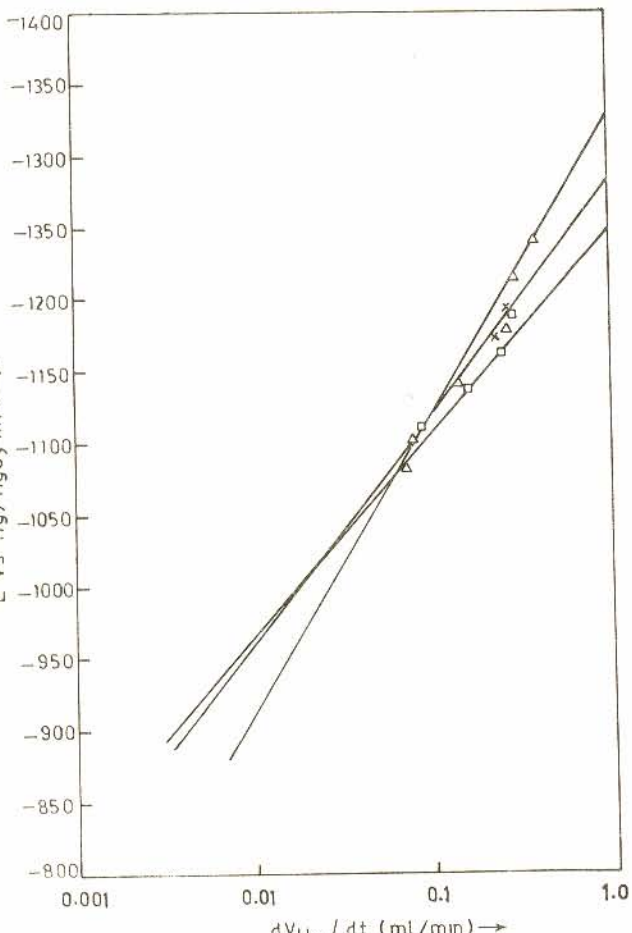

Fig. 3: Applied potential 'E' vs log rate of hydrogen evolution
Δ–Δ Electrode with composition
(Sponge iron + 3% Cu + 15 % Fe_3O_4) powder
X-X (Electrode with composition
(Electrolytic iron powder + 3% Cu + 15% Fe_3O_4)
□-□ *Electrode with composition*
(Water atomised iron powder + 3% Cu + 15% Fe_3O_4)

$$[Cu(OH)_n]^{2-n}_{solution} \longrightarrow Cu_2O + (n-2)\,OH^- + H_2O$$

and

$$Cu_2O + H_2O + 2e^- \longrightarrow 2Cu + 2OH^-$$

The freshly precipitated 'active' copper surface causes a rise in potential for H_2 evolution.

Introduction of Fe_3O_4 to (Fe + 3% Cu) electrode caused the disappearance of peak (III) (ill-defined in Fig. 1). This suggests that the oxidation of Cu to Cu_2O is hindered. The peak potental (IV) was shifted to more noble values. Increase of oxide content enhanced the over-voltage for the process of conversion of $Fe(OH)_2$ to FeOOH. The reason for this retardation could be that Fe_3O_4 is in redox equilibrium with the newly formed $Fe(OH)_2$.

as

$$Fe_3O_4 + 2H_2O + 2e^- \rightleftharpoons Fe(OH)_2 + 2FeO + 2OH^-$$

The presence of Fe_3O_4 reduced the charges flowed under peak V suggesting that the dissolution as divalent soluble Cu is hindered.

Criteria for a battery electrode

The ideal battery electrode requires the reaction

$$Fe(OH)_2 + 2e^- \rightleftharpoons Fe + 2OH^-$$

to proceed reversibly. In TPSV studies the appearance of an anodic peak (II) and the cathodic peak (IX) corresponds to Fe/Fe (II) redox couple [11,12].

$(E_{p,a\,(II)} - E_e) - (E_{p,c\,(IX)} - E_e) = \Delta E_p$. Where ΔE_p is a measure of irreversibility. The more the value of ΔE_p, the more irreversible is the process. As ΔE_p varied linearly wth v, the extrapolation of ΔE_p to zero sweep rate will help in studying the behaviour near revrsible potential. An electrode with $(\Delta E_p)_{v \to 0} = 0$ will exhibit maximum reversibility.

The values of Q_c/Q_a correspond to the charge associated with oxide reduction and the formation of Fe/Fe(II) couple.

TABLE II: Solution analysis for electrolytic iron and electrolytic iron + 3% Cu electrodes in 6 *M* KOH + 0.6 *M* LiOH solutions

Potential applied mV	Dissolved iron mg/lit	Dissolved copper mg/lit
-900	2.0	0.0
-775	1.7	0.0
-525	1.6	0.6
-290	1.5	0.8

TABLE III: Parameters derived from TPSV studies — Effect of source of iron powder, copper and Fe_3O_4 additions

Electrode Composition	Fe/Fe(II) couple $(\Delta E_p)_{v \to 0}$ mV	Fe/Fe(II) couple $\left(\frac{Q_c}{Q_a}\right)_{v \to 0}$
Electrolytic iron + 1% Cu	280	0.92
+ 2% Cu	300	1.00
+ 3% Cu	230	1.33
+ 4% Cu	285	1.44
+10% Cu	265	1.77
+15% Cu	280	1.54
Electrolytic Fe + 3% Cu + 3% Fe_3O_4	225	0.89
+ 10% Fe_3O_4	240	0.88
+ 15% Fe_3O_4	305	0.87
+ 20% Fe_3O_4	235	1.06
Sponge Fe + 3% Cu + 15% Fe_3O_4	270	0.96
Water atomised Fe + 3% Cu + 15% Fe_3O_4	295	0.81

For iron oxide electrodes containing copper peaks II and VII were used to calculate ΔE_p and Q_c/Q_a for reversibility of Fe/Fe(II) redox couple.

Even in solid iron electrodes the values of $(\Delta E_p)_{v \to 0}$ for Fe/Fe(II) couple is 275 mV and this amount of irreversibility is always present as the electrode surface is covered by oxides. An electrode which gives $(\Delta E_p)_{v \to 0}$ values close to that of 275 mV is considered to be the best.

Addition of 3% copper to the electrolytic iron powder gave a value of 230 mV for $(\Delta E_p)_{v \to 0}$ and electrtodes prepard from mixtures of electrolytic iron +3% copper with various amounts of Fe_3O_4 exhibited 205 to 240 mV for $(\Delta E_p)_{v \to 0}$ compared to 275 mV obtained for solid iron and thus favour reversibility of Fe ====>$Fe(OH)_2$ reaction (Table III). When compared to the 295 mV and 270 mV obtained for electrodes 3% Cu + 15% Fe_3O_4 containing water atomised powder and sponge iron powders, electrolytic iron powder + 3% Cu + 15% Fe_3O_4 exhibited 235 mV for $(\Delta E_p)_{v \to 0}$.

The self discharge currents of the electrodes prepared from copper and Fe_3O_4 powders (Table IV) revealed that Fe_3O_4 addition lowered the self discharge of electrolytic iron powder compared to sponge iron powder electrode.This is because of the reduction in i_o for hydrogen evolution [13]. Addition of copper enhances the self discharge of Fe_3O_4 electrodes enhancing the dissolution of iron by galvanic action. However the simultaneous addition of Fe_3O_4 and copper into iron electrodes reduces the self discharge current compared to electrodes from electrolytic iron powder. Sponge iron powder exhibits more self discharge compared to the other electrodes.

TABLE IV: Self discharge current of iron electrode in 6 M KOH + 0.63 M LiOH solutions

Electrode composition	*
Electrolytic iron powder	0.8
Electroltic iron powder + 15% Fe_3O_4	0.2
Electrolytic iron + 3% Cu	1.1
Electrolytic iron powder + 15% Fe_3O_4 + 3% Cu	0.75
Water atomised iron powder + 15% Fe_3O_4 + 3% Cu	0.64
Sponge iron powder + 15% Fe_3O_4 + 3% Cu	1.61

* *Self discharge current mA/g (± 0.1)*

CONCLUSION

Though electrolytic iron powder + 15% Fe_3O_4 electrodes have the least self discharge current, the electrical conductivity of the electrodes are poor compared to electrodes conaining copper powder. Hence electrolytic Fe powder +3% Cu+15% Fe_3O_4 is the optimum composition for iron electrodes for use in Ni-Fe batteries for enhanced conductivity, cycle life and charve retention.

REFERENCES

1. J Labat, J C Jarraisseau and J F Laurent, *Power sources,* D H Collins Edn, **3** (1971) 283
2. V N Flerov, LI Pavlova and LV Uzinger, *Zn Prikl Khim,* **37** (1964) 373
3. V N Flerov, L V Uzinger and LI Pavlova, *Zn Prikl Khim,* **38** (1965) 569
4. I Vogel, *Quantitative Inorganic analysis,* Second Ed, Longman, London (1951) 276
5. G Paruthimal Kalaignan, V S Muralidharan and K I Vasu, *Trans SAEST,* **22** (1987) 67
6. J Cerny and K Micka, *J Power sources,* 25 (1989) 111
7. N Jeyalakshmi and V S Muralidharan, *J Power Sources,* **32** (1990) 277
8. V S Muralidharan and Veerashanmugamani, *J Appl Electrochem,* **15** (1985) 675
9. Pourbaix, *Atlas of Electrochemical equilibria in aqeuous solution,* Pergaomon Press (1966)
10. D W Shoesmith, W Lee, M G Bailey, *Proc Symp on Electrocrystalisation,* Ed, Rolf Weil and R G Barradas, The Electrochemical Society, Pennington **81-6** (1981) 272
11. G Paruthimal Kalaignan, V S Muralidharan and K I Vasu, *J Appl Electrochem,* **17** (1987) 1083
12. G Paruthimal Kalaignan, V S Muralidharan and K I Vasu, *Bull Electrochem,* **4** (1988) 551
13. N Jeyalakshmi and V S Muralidharan, *Proc Indian Acad Sci,* **103** (1991) 753